IOPscience iopscience.iop.org

Home Search Collections Journals About Contact us My IOPscience

The dependence of the interface and shape on the constrained growth of nc-Si in a-SiN_x/a-Si:H/a-SiN_x structures

This article has been downloaded from IOPscience. Please scroll down to see the full text article.

2002 J. Phys.: Condens. Matter 14 10083

(http://iopscience.iop.org/0953-8984/14/43/307)

View the table of contents for this issue, or go to the journal homepage for more

Download details:
IP Address: 171.66.16.96
The article was downloaded on 18/05/2010 at 15:16

Please note that terms and conditions apply.

J. Phys.: Condens. Matter **14** (2002) 10083–10091 PII: S0953-8984(02)32779-6

The dependence of the interface and shape on the constrained growth of nc-Si in a-SiN_x/a-Si:H/a-SiN_x structures

Lin Zhang, Kai Chen, Li Wang, Wei Li, Jun Xu, Xinfan Huang and Kunji Chen[1]

National Laboratory of Solid State Microstructures and Department of Physics, Nanjing University, Nanjing 210093, People's Republic of China

E-mail: kjchen@netra.nju.edu.cn

Received 16 January 2002, in final form 22 July 2002
Published 18 October 2002
Online at stacks.iop.org/JPhysCM/14/10083

Abstract
Size-controlled nanocrystalline silicon (nc-Si) has been prepared from a-SiN_x/a-Si:H/a-SiN_x ('a' standing for amorphous) structures by thermal annealing. Transmission electron microscope analyses show that the lateral size of the nc-Si is controlled by the annealing conditions and the a-Si sublayer thickness. The deviation of the nc-Si grain size distribution decreases with the a-Si sublayer thickness, so thinner a-Si sublayers are favourable for obtaining uniform nc-Si grains. In the a-Si:H (10 nm) sample annealed at 1000 °C for 30 min, an obvious bi-modal size distribution of nc-Si grains appears, but no obvious bi-modal size distribution is found in other samples with thinner a-Si:H sublayers. On the basis of the experimental results, we discuss the process of transition from the sphere-like shape to the disc-like shape in the growth model of the nc-Si crystallization. The critical thickness of the a-Si sublayer for the constrained crystallization can be determined by the present model. Moreover, the increase of the crystallization temperature in the ultrathin a-Si sublayer is also discussed.

(Some figures in this article are in colour only in the electronic version)

1. Introduction

Room temperature light emission from silicon has been shown to be possible when Si is in the form of a low-dimensional system [1–4]. Low-dimensional systems, such as nanocrystalline silicon (nc-Si), are currently being studied to identify new applications in both nanoelectronic and photoelectronic devices [5]. A key issue is control of the grain size and the grain size

[1] Author to whom any correspondence should be addressed.

 © 2002 IOP Publishing Ltd Printed in the UK

distribution (GSD) [6]. Recent studies revealed that the nc-Si size could be controlled by the sublayer thickness in multilayers [7, 8]; this was based on the constrained growth of nc-Si when the a-Si layer thickness was ultrathin (<10 nm). The process of nucleation and growth of nc-Si from the amorphous phase in an ultrathin layer by laser or thermal annealing is quite different from that for bulk silicon. Until now, the mechanism of crystallization of a-Si in ultrathin layers has not been fully understood [9]. In addition, the crystallization temperature increased extraordinarily with decrease in the a-Si sublayer thickness [10, 11]. How can one explain this extraordinary crystallization phenomenon? The previously reported model for nc-Si growth was derived from the Gibbs free energy of a crystallite between two interfaces according to the classical nucleation theory. The halt in growth of nc-Si occurred when the gradient of the free energy change was positive, but this finding is only qualitative and there is a lack of exact experimental data on the interfacial free energy [12].

In our previous work, a method of laser-induced constrained crystallization of ultrathin a-Si:H sublayers within a-SiN_x/a-Si:H multilayers was adopted to fabricate nc-Si grains [13, 14]. Visible and stable photoluminescence [15] and electroluminescence [16] have been observed at room temperature from the nc-Si grains prepared by this method.

In this paper, we focus on the influence of the thermal annealing conditions and the a-Si sublayer thickness on the size and shape of the nc-Si. We modify Tagami and Persans' model [12, 17] of nucleation and growth of nc-Si, and discuss quantitatively the effects of the interface and shape of the nc-Si on the crystal growth in relation to the Gibbs free energy.

2. Experiments

The a-SiN_x/a-Si:H/a-SiN_x samples were deposited on substrates of quartz at 250 °C by a computer-controlled plasma-enhanced chemical vapour deposition (PECVD) system. During the deposition, the SiH_4 gas was decomposed with a rf power of 30 W to fabricate amorphous silicon. The a-Si:H sublayer thicknesses were 4, 7 and 10 nm. Insulating a-SiN_x:H was made from a gas mixture consisting of $NH_3/SiH_4 = 5$ (volume ratio), and the a-SiN_x:H sublayer thickness was kept to 30 nm. The crystallization of samples was performed by furnace annealing at 1000 °C in a N_2 atmosphere for 30 or 120 min. The microstructures of the samples after thermal annealing were investigated by planar and cross-section transmission electron microscope (TEM) measurements.

3. Results

Figure 1 presents the planar dark-field (DF) TEM micrographs and the corresponding GSDs of a-Si:H (4 nm), a-Si:H (7 nm) and a-Si:H (10 nm) samples annealed at 1000 °C for 30 min. The nucleation sites of the nc-Si grains are random. From figures 1(d)–(f), the average grain sizes of a-Si:H (4 nm), a-Si:H (7 nm) and a-Si:H (10 nm) samples are 5.0 ± 2.5, 8.0 ± 3.5 and 10.3 ± 6.5 nm, respectively. It is seen that the deviation of the nc-Si GSD decreases with the a-Si sublayer thickness, so thinner a-Si sublayers may be favourable for obtaining uniform nc-Si grains. The longitudinal size of the nc-Si is equal to the a-Si sublayer thickness, because the a-SiN_x sublayer can prevent nc-Si grains from growing. From the GSDs, the maximum lateral size of nc-Si is about double the a-Si sublayer thickness. Therefore, the larger nc-Si grains can be regarded as having a disc-like shape. In addition, we found the obvious bi-modal size distribution shown in figure 1(f), but no bi-modal distribution in other samples. In fact, the bi-modal size distribution corresponds to two growth stages of nc-Si [18]. The size distribution of the larger grains corresponds to nucleation and growth of nc-Si in the first stage.

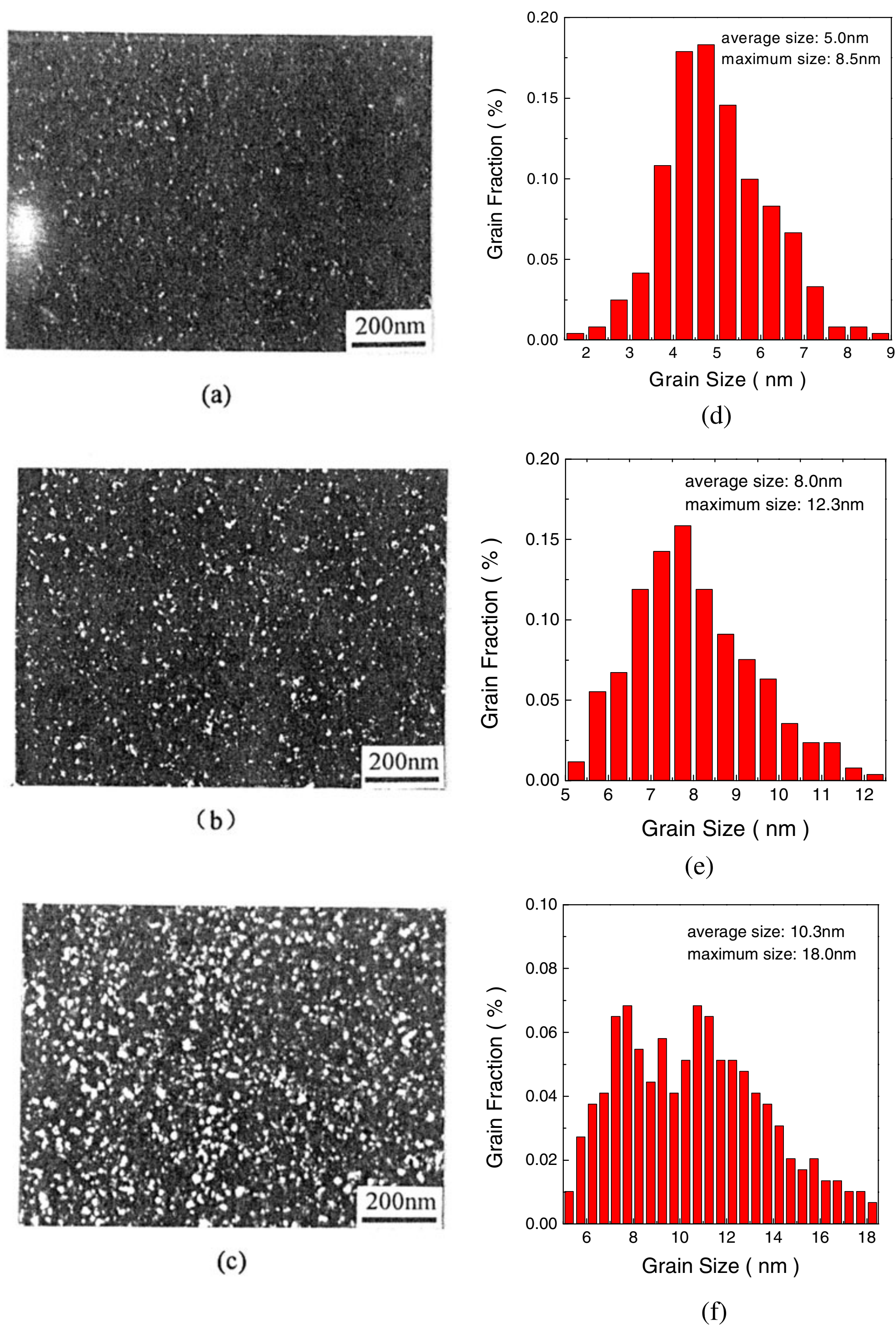

Figure 1. Planar TEM micrographs of the samples annealed at 1000 °C for 30 min, and the corresponding GSDs; (a) a-Si:H (4 nm); (d) the GSD of (a); (b) a-Si:H (7 nm); (e) the GSD of (b); (c) a-Si:H (10 nm); (f) the GSD of (c).

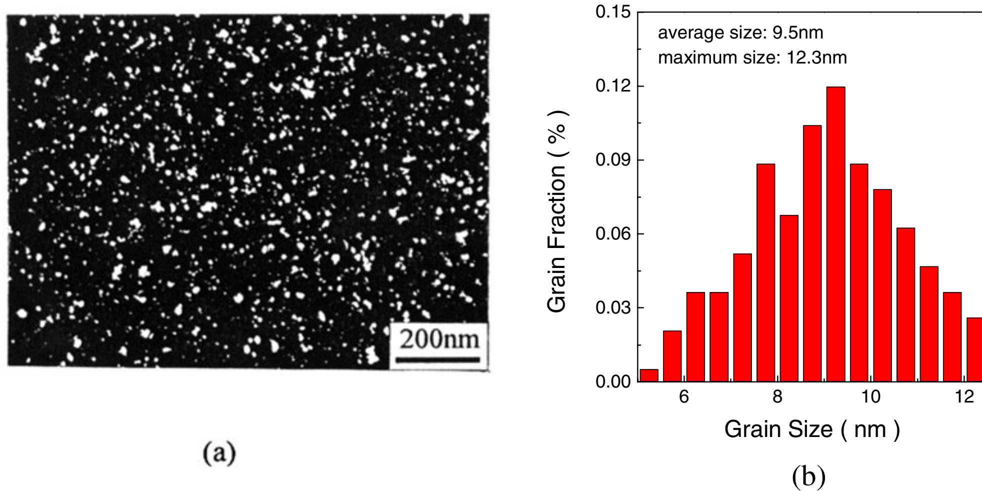

Figure 2. (a) A planar TEM micrograph of the a-Si:H (7 nm) sample annealed at 1000 °C for 120 min; (b) the corresponding GSD.

After nucleating, the nc-Si grains will grow to the bigger size due to the lower grain density in the first stage. When an nc-Si grain has grown to a certain size, its growth will be constrained by the interface; then the new nc-Si nuclei will appear. In this growth process, the latter nuclei will be affected by the former nc-Si grains. The latter grains only exist in the space between the former grains, so they are smaller than those formed in the first stage. The size distribution of the larger grains may be close to the thermodynamic equilibrium state. In the thicker a-Si:H sublayer (10 nm), the space between grains formed in the first stage is much bigger than that in the thinner a-Si:H sublayer, so there is enough space for the new nc-Si grains to nucleate and grow. Due to the lack of space, stress field and interface, it is difficult for the nc-Si grains to nucleate and grow in the ultrathin film, and only one size distribution exists.

Figure 2 presents the planar DF TEM micrograph and the corresponding GSD for a-Si:H (7 nm) sample annealed at 1000 °C for 120 min. The average grain size is 9.5 ± 2.8 nm. Here no obvious bi-modal size distribution appears. Comparing figure 2(b) with figure 1(e), we see that the average grain size of nc-Si increases with the annealing time, but the maximum lateral sizes of the nc-Si for these two samples are both 12.3 nm. This indicates that the nc-Si grains grow to a certain size, then stop growing. This phenomenon reflects the characteristic of constrained growth of grains in the ultrathin layer. Here, we may consider the maximum lateral size of nc-Si to be the thermodynamic equilibrium size.

Figure 3 shows a cross-section TEM image of the a-Si sublayer in which the lattice fringe of a nc-Si grain is observed. The nc-Si grain with clear $\{111\}$ lattice planes is embedded in the a-Si matrix. According to the cross-section and planar TEM images, the larger nc-Si grains must be disc-shaped.

4. Growth model

How do we explain the constrained growth of nc-Si? According to the above experimental results, the processes of nucleation and growth of nc-Si can be schematically described as in figure 4(a). The nc-Si grain is changed from the sphere-like shape to the disc-like shape. This model is fairly suitable for the crystallization of the ultrathin a-Si sublayer with the lower

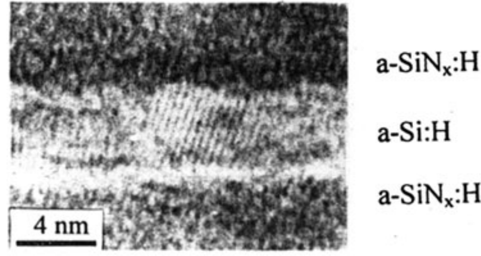

Figure 3. A cross-section TEM image of the a-Si sublayer.

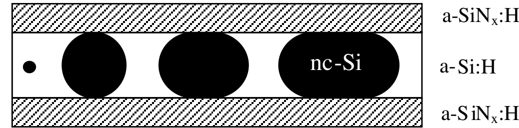

(a)

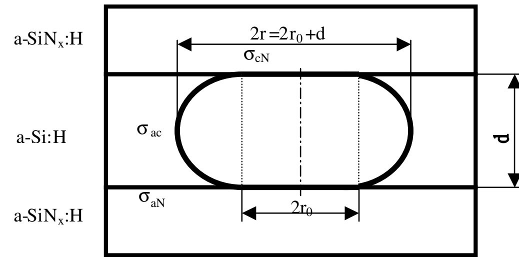

(b)

Figure 4. (a) The scheme for the processes of nucleation and growth of nc-Si. (b) The cross-section shape of the larger nc-Si grains.

grain density since there is low crystallinity and less agglomeration of nc-Si grains in this case. Otherwise, the grains start to touch each other and grow into a brick-like shape [8, 19]. The change of the grain shape from sphere-like to disc-like is supported by the cross-section TEM images, as shown in figure 3. When the grain shape becomes disc-like, the energy of the interface between nc-Si and a-SiN$_x$ appears; this increases the growth free energy of nc-Si and finally causes the growth to halt. Therefore, we discuss nc-Si growth on the based of the grain shape and the interfacial energy.

The free energy change accompanying the formation of a spherical crystallite in the amorphous layer, ΔG_1, is given by

$$\Delta G_1 = -\tfrac{4}{3}\pi r^3\,\Delta G_{ac} + 4\pi r^2\sigma_{ac} \tag{1}$$

where r is the radius of the crystallite. ΔG_{ac} is the free energy change per unit volume in the amorphous-to-crystalline phase transition, which can be determined from the specific heat difference between amorphous and crystalline silicon [20]. ΔG_{ac} at 1000 °C is about 8.85 eV nm^{-3} (0.177 eV/atom). σ_{ac} ($\sim$1.46 eV nm^{-2} or 0.1075 eV/atom) is the interfacial free energy per unit area for the interface between amorphous and crystalline Si [21]. As the spherical nc-Si grains start to come into contact with the a-SiN$_x$ sublayer, the crystallites may be presumed to be disc-like grains, as shown in figure 4(b). The free energy change of the

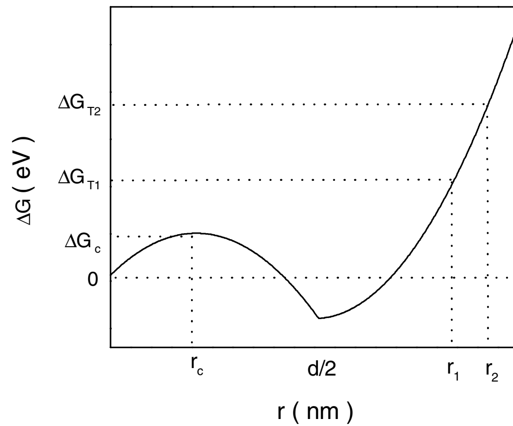

Figure 5. A schematic diagram of the free energy change of nc-Si accompanying the crystallization process.

disc-like grains, ΔG_2, can be expressed as

$$\Delta G_2 = -V\,\Delta G_{ac} + S_1\sigma_{ac} + S_2(\sigma_{cN} - \sigma_{aN}) \tag{2}$$

where V is the volume of the disc-like grains: $V = \pi d^3/6 + \pi d r_0^2 + \pi^2 r_0 d^2/4$; S_1 and S_2 are the surface areas of the disc-like grains: $S_1 = 2\pi r_0^2$, $S_2 = \pi^2 d^2/4 + 2\pi d r_0$; d is the a-Si sublayer thickness; r and r_0 are shown in figure 4(b). σ_{cN} is the free energy of the interface between the nc-Si and a-SiN_x per unit area and σ_{aN} is the free energy of the interface between a-Si and a-SiN_x per unit area.

5. Discussion

Using the above growth model of nc-Si, we first analyse the constrained growth of nc-Si qualitatively. Figure 5 shows schematically the free energy change of the nc-Si grains accompanying the growth process. From equations (1) and (2), the free energy change of nc-Si is ΔG_1 when $r < d/2$, while the free energy change of nc-Si is ΔG_2 when $r > d/2$. According to the previously reported model [12, 17], the growth halt for nc-Si occurs when $\partial\,\Delta G(r)/\partial r$ is positive. From the thermodynamic theory, we can estimate whether the continuous growth of the grain needs external energy by $\Delta G(r)$ rather than $\partial\,\Delta G(r)/\partial r$. In fact, the nc-Si grains can grow continuously when $\Delta G(r) < 0$. Therefore, $\Delta G(r)$ can be considered as a criterion for constrained crystallization in our present model of nc-Si growth. In this paper, we mainly study the thermodynamic equilibrium process of the constrained growth of nc-Si, and the halt in growth of nc-Si always occurs when $r > d/2$, so our present model is suited to this case because its results agree with the experimental results.

The free energy change is difficult to measure directly, but it can be estimated by the energy needed for a-Si crystallization. When the external energy caused by improving the temperature is lower than the crystallization energy needed, the halt in growth of nc-Si will occur. Here, the external energy ΔG_T may be tentatively estimated in accordance with Boltzmann's law [22]. The dependence on the external energy ΔG_T of the annealing temperature T is described as follows:

$$\Delta G_T = ckT \tag{3}$$

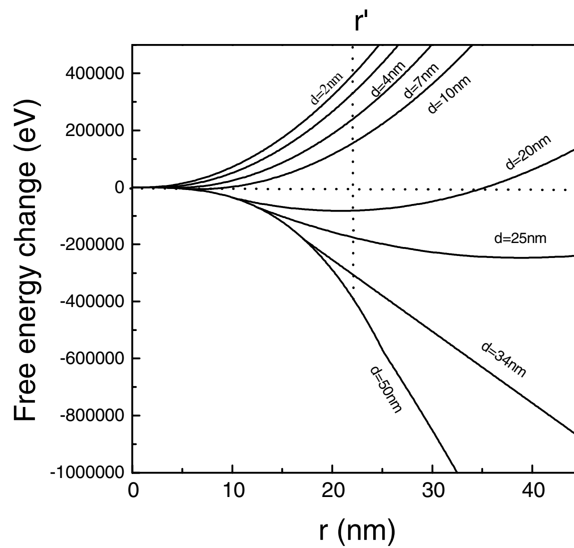

Figure 6. The free energy change dependence of the nc-Si grain radius at various thicknesses of a-Si sublayers.

where c is a constant and k is Boltzmann's constant. In the disc-like nc-Si growth process, the free energy change of nc-Si increases with the interfacial free energy. When the free energy change ΔG_2 reaches the external energy ΔG_T, the nc-Si grains will stop growing. As shown in figure 5, nc-Si grains with maximum lateral radii of r_1 and r_2 require the external energies ΔG_{T1} and ΔG_{T2}, respectively. The thermodynamic equilibrium size of nc-Si increases with the annealing temperature.

In order to analyse quantitatively the constrained crystallization of nc-Si in relation to the Gibbs free energy, ΔG_{ac}, σ_{ac} and $\Delta\sigma$ (here, $\Delta\sigma = \sigma_{cN} - \sigma_{aN}$) must first be determined from equation (2). ΔG_{ac} and σ_{ac} are available, but the increment of the free energy of the interface between nc-Si and a-SiN$_x$, $\Delta\sigma$, is unknown. Here, we try to use our experimental results to calculate the $\Delta\sigma$ value. In the thermodynamic equilibrium state, the free energy change ΔG_2 is equal to the external energy ΔG_T, and the grain size has reached the maximum size. At the annealing temperature of 1000 °C, ΔG_2 and ΔG_T remain constant. According to equation (2), we may choose two experimental results to determine the $\Delta\sigma$ value. Here, the maximum lateral size of nc-Si is used to replace the thermodynamic equilibrium size. From the statistical results in figure 1, when the a-Si sublayer thickness d is 4 nm, r_0 is 1.8 nm; when d is 10 nm, r_0 is 4.0 nm. From equation (2), the value of $\Delta\sigma$ is 151.1 eV nm^{-2}. $\Delta\sigma$ is much bigger than σ_{ac}, so the free energy of the interface between nc-Si and a-SiN$_x$ may play an important role in the nc-Si growth process. It is difficult for nucleation to occur at the interface between the a-Si:H sublayer and the a-SiN$_x$ sublayer due to the bigger interfacial free energy; thus the nucleation of nc-Si can only occur within the a-Si sublayer, which agrees with our present model, as shown in figure 4(a).

Now, the free energy change of the nc-Si growth can be calculated quantitatively using $\Delta\sigma$. Figure 6 shows the free energy change dependence of the nc-Si grain radius r (here, $r = r_0 + d/2$) at various thicknesses of a-Si sublayers. From equation (2), $\Delta G_2(r)$ is a parabolic function of r. When $-\pi d\,\Delta G_{ac} + 2\pi\,\Delta\sigma = 0$, $\Delta G_2(r)$ is a line. Then, a threshold thickness d_0 of the a-Si sublayer can be obtained:

$$d_0 = 2\,\Delta\sigma/\Delta G_{ac}. \tag{4}$$

Here, the threshold thickness is about 34 nm. When the thickness of the a-Si sublayer $d < d_0$, $\Delta G_2(r)$ is an upward parabolic function, and the free energy change of the nc-Si grain increases with the nc-Si grain size. While $d > d_0$, $\Delta G_2(r)$ is a downward parabolic function, and the free energy change decreases rapidly with increasing grain size. Therefore, the threshold thickness d_0 can be considered as the critical thickness of the a-Si sublayer where the growth of nc-Si can be constrained and stopped thermodynamically. In other words, the constrained crystallization of a-Si:H may only occur when the a-Si sublayer thickness is below d_0.

The a-Si sublayer thickness also plays an important role in the constrained crystallization, as we see from figure 6. As the nc-Si lateral radius is r', as shown in figure 6, the free energy change of the nc-Si growth $\Delta G_2(r)$ will increase gradually with decreasing a-Si sublayer thickness; then the external energy needed for the nc-Si growth and the crystallization temperature will also increase with decreasing a-Si sublayer thickness. When the a-Si sublayer is thinner, the surface/volume ratio of the grains will increase, so the interfacial free energy will be much more important to the nc-Si growth. From above analyses, we found that the extraordinary increase of the crystallization temperature in the ultrathin a-Si sublayer is mainly caused by increasing the interfacial free energy. Once the nc-Si grain has grown to a certain size and the free energy change $\Delta G_2(r)$ has become bigger than the external energy ΔG_T, the halt in growth of nc-Si in the a-Si sublayer will occur in the lateral direction. On the basis of the mechanism of the constrained growth of nc-Si, we may control the nc-Si sublayer thickness and the annealing conditions to prevent nc-Si grains from growing; then size-controlled and uniform nc-Si grains will be obtained.

6. Conclusions

Size-controlled nc-Si can be prepared from a-SiN_x/a-Si:H/a-SiN_x structures by thermal annealing. The lateral size of the nc-Si is controlled by the annealing conditions and the a-Si sublayer thickness. The deviation of the nc-Si GSD decreases with the a-Si sublayer thickness, so thinner a-Si sublayers are favourable for obtaining uniform nc-Si grains. The maximum lateral grain size of nc-Si is about double the a-Si sublayer thickness, and it is the critical size for the nc-Si growth being halted thermodynamically. The mechanism of the constrained growth of nc-Si has been studied in accordance with the classical thermodynamic theory. The interfacial free energy will increase and become much more important to the nc-Si growth with decreasing a-Si sublayer thickness. The extraordinary increase of the crystallization temperature in the ultrathin a-Si sublayer is mainly caused by increasing interfacial free energy. In addition, the critical thickness of the a-Si sublayer for the constrained crystallization can be determined from our present model.

Acknowledgments

This work was supported by the National Natural Science Foundation of China under grant Nos 69890225, 60071019 and in part by Korea Ministry of Science and Technology through the TLND Project.

References

[1] Lu Z H, Lockwood D J and Baribeau J M 1995 *Nature* **378** 258
[2] Wilson W L, Szajowski P F and Brus L E 1993 *Science* **262** 1242
[3] Furukawa S and Miyasato T 1988 *Phys. Rev.* B **38** 5726
[4] Takagi H, Ogawa H and Yamazabi Y 1992 *Appl. Phys. Lett.* **56** 2379

[5] Pavesi L, Negro L D and Mazzoleni C 2000 *Nature* **408** 440
[6] Photopoulos P, Nassiopoulou A G and Kouvatsos D N 2000 *Mater. Sci. Eng.* B **69–70** 345
[7] Chen K J, Huang X F and Xu J 1993 *J. Non-Cryst. Solids* **164–166** 977
[8] Grom G F, Lockwood D J and McCaffrey J P 2000 *Nature* **407** 358
[9] Robertson J 2000 *J. Non-Cryst. Solids* **266–269** 79
[10] Zacharias M, Blasing J and Veit P 1999 *Appl. Phys. Lett.* **74** 2614
[11] Zacharias M, Blasing J and Hirschman K 2000 *J. Non-Cryst. Solids* **266–269** 640
[12] Tagami T, Wakayama Y and Tanaka S 1997 *Japan. J. Appl. Phys.* **36** L734
[13] Chen K J, Huang X F, Xu J and Feng D 1996 *J. Non-Cryst. Solids* **198–200** 833
[14] Chen K J, Huang X F, Xu J and Feng D 1992 *Appl. Phys. Lett.* **61** 2069
[15] Huang X F, Li Z F, Liu Z G and Chen K J 1996 *J. Non-Cryst. Solids* **198–200** 821
[16] Wang M X, Huang X F and Chen K J 1998 *Appl. Phys. Lett.* **72** 722
[17] Persans P D, Ruppert A and Abeles B 1988 *J. Non-Cryst. Solids* **102** 130
[18] Yakayama Y, Tagami T and Tanaka S 1999 *Thin Solid Films* **350** 300
[19] Chae K H, Son J H and Chang G S 1999 *Nanostruct. Mater.* **14** 1239
[20] Kumomi H and Yonehara T 1994 *J. Appl. Phys.* **75** 2884
[21] Spinella C, Lombardo S and Priolo F 1998 *J. Appl. Phys.* **84** 5383
[22] Honma I, Komiyama H and Tanaka K 1989 *J. Appl. Phys.* **66** 1170